Miscibility Determination of a Lower Critical Solution Temperature Polymer Blend by Rheology

Jitendra Sharma* and Nigel Clarke

Department of Chemistry, Science Site Laboratories, University of Durham, South Road, Durham DH1 3LE, U.K.

Received: April 2, 2004; In Final Form: June 28, 2004

Rheology on a miscible blend of deuterated polystyrene (PSD) and poly(vinyl methyl ether) (PVME) is reported in the temperature range of T_g (glass-transition temperature) + 45 K to T_g + 155 K, extending from homogeneous to the two-phase region of the blend's phase behavior. Data obtained from rheology, performed in different modes of applied shear, has been used to determine the miscibility range of this particular blend system. Phase separation temperature and the region of miscibility are determined from the dynamic temperature sweep experiment carried out in the parallel plate geometry. While the binodal temperature is marked by the first change in the slope of the storage modulus and the peak, in the tan δ curve, miscible and phase-separated regions are identified as the off-peak zones. Shift factors obtained from the time−temperature superposition (tTS) exhibit Williams−Landel−Ferry (WLF) behavior in the homogeneous region. Thermorheological complexity observed through the failure of tTS and deviation from temperature independence of Han plots in the terminal region near the phase boundary suggests the onset of phase separation in the rheologically identified metastable region. In addition to the qualitative analysis of the temperature-dependent viscosity data (in the linear viscoelastic regime) where the observed departure in viscosity−temperature relationship is interpreted as signature of spinodal decomposition, quantitative analysis of the shear rheological data based on mean-field theory has been used to determine the spinodal temperature of the PSD/PVME blend system. The estimated correlation length, near the critical region, exhibits divergence caused by enhanced concentration fluctuations. However, Onuki's prediction of viscosity enhancement at high shear rates near the critical region, a characteristic associated with phase separation in two-component systems, could not be observed for the PSD/PVME blend.

1. Introduction

The rheology of miscible and partially miscible polymer blends has long attracted the interest of the scientific and industrial community.[1−9] The applicability of amorphous polymers can be increased significantly by blending suitably with polymers of varying T_g (glass-transition temperature), thus providing an easy route to making new materials with desired properties.[10,11] Exhibiting lower critical solution temperature (LCST) behavior,[12] blends of polystyrene (PS) and poly(vinyl methyl ether) (PVME) have been studied extensively in terms of their behavior toward phase equilibria,[11−13] phase-separation kinetics and resulting morphologies,[13−18] temperature and composition dependence[19,20] and the pressure dependence[21] of the Flory−Huggins interaction parameter, and rheology.[3−9] A different kind of phase behavior for the blends of PS/PVME has been reported under quiescent and flow conditions. While a mean-field to Ising transition of the concentration fluctuations close to the critical temperature has been observed under quiescent conditions,[22] interesting phenomena of shear-induced mixing (SIM) and demixing (SID) occurred when flow fields were applied.[23−26] Apart from the molecular weight of the constituent components affecting the miscibility window, a huge difference in the glass-transition temperature of the components of the order ca. 125 K introduces dynamic asymmetry, leading to the process known as "viscoelastic phase separation", in the blends of PS/PVME.[27] With a negative enthalpy of mixing,[28,29] and a small negative volume change on mixing,[29,30] blends of PS/PVME possess a slightly negative value for the Flory−Huggins interaction parameter.[31,32] All these combined with a large difference in the glass-transition temperature of the components contribute to the thermorheological complexity of this particular blend.[33] The empirical time−temperature superposition (tTS) principle[34] breaks down for such miscible blends with very different glass-transition temperatures, manifesting a complex rheological behavior.[2,35−39] Blends of PS/PVME are found to exhibit thermorheologically complex behavior at both the terminal and the segmental levels as probed by oscillatory shear and dielectric response, respectively.[4] The thermorheological complexity of miscible binary blends is also evident from the fact that there exists no general rule to predict the viscosities of binary blends even with the prior knowledge of monomeric friction coefficients of the constituent components.[40]

Most aspects of the rheological study on the PS/PVME blend often deal with the case when hydrogenous polystyrene PSH (being a natural choice) has been used as one component. In a number of studies,[21,22,41−45] where the behavior of the blend has been investigated on smaller length scales, small-angle neutron scattering (SANS) is used which requires replacing hydrogenous polystyrene, PSH, with deuterated polystyrene, PSD, in order to achieve contrast in these experiments, and assuming a negligible effect on the values of the thermodynamic interaction parameters. Though the LCST of the PS/PVME

* Corresponding author. E-mail: Jitendra.Sharma@durham.ac.uk.

10.1021/jp048552h CCC: $27.50
Published on Web 08/07/2004

TABLE 1: Characteristics of the Polymers Used in the Experiment

sample	M_w	M_w/M_n	T_g (°C)
PSD	38300	1.03	~105
PVME	23700	4.26	−46.0
PSD/PVME			−4.5

blend largely depends on the component molecular weights,[13] studies reveal that the thermodynamics is affected significantly as a result of this replacement. While the glass-transition temperature remains unaffected, the LCST can apparently be raised by approximately 40 °C.[30] Similar observations have been reported earlier using fluorescence techniques.[46] For an equal degree of superheating,[47] the kinetics of phase separation for PSD/PVME blends is about 10 times faster than that for the PSH/PVME blends.[30] In view of the above observations and the fact that the thermodynamics of the blend is affected significantly by the choice of deuterated or hydrogenous polystyrene as one component, separate investigations on the rheological aspects of a PSD/PVME blend have been carried out.

Experiments reported in this paper consist of different type of rheological measurements performed on a high molecular weight 50:50 (wt/wt %) blend of PSD and PVME in different modes of applied shear in order to determine the miscibility range of the blend from experiments based purely on rheology.

2. Experimental Section

Materials. Samples of PVME in water (50 wt % of solute) obtained from Aldrich Chemical Co. were vacuum-dried at room temperature for 48 h before being used for the preparation of deuterated polystyrene/poly(vinyl methyl ether) (PSD/PVME) blends. Polystyrene-d_8 (PSD) used for the blend was synthesized in the laboratory using standard techniques of anionic polymerization of styrene-d_8 in benzene with *sec*-butyllithium as an initiator.[48] Gel permeation chromatography (GPC) performed using THF as solvent was used to determine the weight-average molecular weights (M_w) of the PSD and PVME and their polydispersities (M_w/M_n), where M_n is the number-average molecular weight. The weight-average molecular weights and the molecular weight distributions thus found were 38300 and 1.03 for PSD and 23700 and 4.26 for PVME (see Table 1). The quantities reported are determined using the calibration curve of narrow distribution polystyrene standards. From here onward in this literature, blends prepared from the above polymers with the aforesaid individual molecular weights will be referred to as PSD-38K/PVME-23K blend. The molecular weights of both PSD and PVME were chosen to ensure that they remain reasonably entangled. Owing to the chemically sensitive nature of PVME, utmost care was taken in the blend preparation and to prevent it from oxidation. This can also be ensured by a simple visual observation of the blends looking transparent with a slightly yellowish hue. Any degradation will be revealed by a change in the color of the sample.

Blends of PSD-38K/PVME-23K used in the experiment were prepared from the ternary solution of PSD and PVME in toluene. The mixed solution was left at room temperature for 2 days to allow solvent evaporation followed by drying under vacuum at ca. 70 °C for a week. Complete evaporation of the solvent from the blends was ensured by weighing the sample continuously and making the values match asymptotically to the total weight of the components. The dried sample was then compression-molded at T_g + 70 °C into sheets of ~1 mm thickness. The blends so prepared had a transparent look. PVME is known to be hygroscopic in nature and can absorb moisture and alter the overall nature of the blend and its phase behavior. Repeat measurements of viscoelastic properties were made after the experiments to ensure that the blends studied represented the true nature of the blend free from moisture exposure or degradation effects.

Methods. The viscoelastic properties of the blends were measured by shear rheology in different modes of applied stress on a Rheometric Scientific SR5 stress-controlled rheometer, equipped with a force-rebalance transducer and an environmental temperature-controller with the measurement accuracy of ±0.1 °C. All experiments were carried out in parallel-plate geometry with plate fixtures of size 25 mm in diameter. Isothermal frequency sweep curves of the storage and loss modulus were measured in the temperature range of T_g + 45 °C to T_g + 155 °C with the angular frequency (ω) varied from 0.05 to 500 rad/s. The range of temperatures covered in the study probed the entire region of the blend's phase behavior, extending from homogeneous to the two-phase regime of the phase diagram. A strain of amplitude 0.05 was applied to ensure that the measurements fall well within the linear viscoelastic regime. Effects of temperature on the viscoelastic response of the blends were also studied by (i) isochronal dynamic temperature sweep experiment, carried out by the measurement of the storage and loss modulus at a fixed frequency of 1 rad/s and a uniform rate of heating (0.4 °C/min); and (ii) temperature sweep experiment, in which viscosity measurement of the blend was carried out in the linear viscoelastic regime (at vanishing small shear rate, 5×10^{-2} s^{-1}) and with a uniform temperature increment (0.5 °C/min) while the system undergoes transition from the homogeneous to the phase-separated region of the phase diagram.

Thermal analysis and the glass-transition temperature (T_g) determination of the PSD-38K/PVME-23K blends were carried out by thermal-gravimetric analysis (TGA) and differential scanning calorimetry (DSC) respectively on Perkin-Elmer (Pyris 1) instruments. Prior to DSC measurements, the instrument was calibrated using standard materials of known melting point temperatures. For each DSC measurement on PSD-38K/PVME-23K blends, a specimen of 15 mg of the sample was first heated to T_g + 100 °C at a heating rate of 10 °C/min; annealed for 5 min; and then quenched to T_g − 75 °C at a cooling rate of 200 °C/min. A second heating at a rate of 10 °C/min was used to determine the T_g (taken normally as the temperature in the middle of the transition curve) of the specimen. TGA of the blend performed in the temperature range from ambient to 300 °C was also carried out at a heating rate of 10 °C/min.

3. Results

3.1. Thermal Analysis. DSC traces obtained from blends of PSD-38K/PVME-23K exhibited a glass-transition temperature intermediate to the glass-transition temperature of the pure components. The thermogram obtained from a 50:50 composition of this blend exhibited a single calorimetric glass-transition temperature of −4.5 °C, within a transition spectrum of width approximately 25 °C. Blends exhibiting a single glass-transition temperature (T_g) are often regarded as miscible while the immiscible ones are characterized by two distinct values of the T_g, corresponding to the compositions of the two phases.[10] Features of single T_g and the optical transparency of the blends were considered as necessary and sufficient evidence for the miscibility of the blend. In certain cases, when the observed single glass-transition temperature is very broad [e.g., Schneider and Wirbser observed such transitions to occur over a temper-

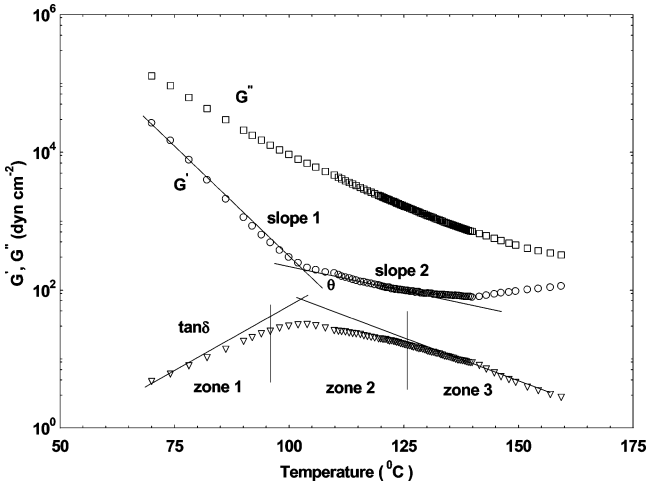

Figure 1. Isochronal ($\omega = 1$ rad/s) dynamic temperature sweep of storage modulus G', loss modulus G'', and the loss tangent, tan δ, for a 50:50 PSD-38K/PVME-23K blend obtained at constant applied strain of 0.05. The rheologically determined phase separation (binodal) temperature ($T_b \cong 104$ °C) is marked in the figure, where the first change in the slope of the smoothly varying G' curve occurs at a heating rate of 0.5 °C/min. The three different zones shown in the figure correspond to the miscible (zone 1; $T \lesssim 96$ °C), metastable (zone 2; 96 °C $\lesssim T \lesssim$ 125 °C), and phase-separated (zone 3; $T \gtrsim 125$ °C) regions of the phase diagram. The two solid lines, representing slope of G', are guides to eye only and are not actual fits to the experimental data. The magnitude of the upturn in G', estimated by angle $\theta = \tan^{-1}$(slope 2) $- \tan^{-1}$(slope 1), is 3.6°.

ature range of approximately 60 °C for the blends of polystyrene (PS)/poly(vinyl methyl ether)(PVME)],[6] dynamic mechanical thermal analysis (DMTA) has been argued as being more sensitive in the T_g determination of the blends than DSC,[49] because DMTA can resolve the size of domains (or pseudo phase-separated regime) over a 5−10 nm scale as has been studied by Molnar et al.[50] for the blends of polyamide-6 (PA-6) with sulfonated polystyrene ionomers through the observed peak in the tan δ curve. The ability to detect a single or double transition in a two-phase system by an instrument has been studied through a compatibility parameter N_c, which is the ratio of experimental probe resolution scale to the domain size of the phase, and the dimension for the DMTA resolution is of the order 15−30 nm.[51] While NMR techniques can detect composition fluctuations in the dimensional range of 2.5−5 nm,[52] SANS has been used frequently to study these fluctuations over a 0.5−100 nm scale.[21,22,41−45] The observed glass transition for the PSD-38K/PVME-23K blends studied here extended only over a temperature range of approximately 25 °C, less than half the value observed by Schneider and Wirbser.[6] Therefore, DSC can adequately determine T_g of blends in our case. A possible reason for observing such a narrow range of glass-transition temperature here could be the use of deuterated polystyrene when the concentration fluctuations are suppressed due to the stronger negative enthalpy of mixing. The glass-transition temperatures of the blend and its constituent components PSD and PVME are listed in Table 1 alongside their individual molecular weights and polydispersities. TGA on the blends of PSD-38K/PVME-23K exhibited a fairly stable behavior within the range of temperatures extending from homogeneous to the two-phase regime of the blend with the ceiling temperature being around 155 °C.

3.2. Oscillatory Shear Measurements. *3.2.1. Isochronal Dynamic Temperature Sweep Experiment.* Figure 1 shows temperature sweep of G' and G'' for a 50:50 PSD-38K/PVME-23K blend at a constant frequency of $\omega = 1$ rad/s and an overall heating rate of 0.5 °C/min when the applied strain amplitude is 0.05. A uniform decrease in the magnitude of the storage modulus is observed up to temperature $T \approx 96$ °C followed by a region where the decrease in G' slows down drastically. This is clear from the observed change in the slope of the G' curve at $T \cong 104$ °C shown by the intersection of two slopes in the figure. The magnitude of upturn in the G' behavior can be estimated from the value of θ (shown in Figure 1), where $\theta = \tan^{-1}$(slope 2) $- \tan^{-1}$(slope 1), and the two slopes of the G' curve refer to the ones before and after the upturn. The value of θ for a 50:50 PSD-38K/PVME-23K blend estimated from the difference in the slopes of the G' curve (as shown in Figure 1) is 3.6°. The magnitude of the upturn and the temperature range over which it occurs strongly depend on the dynamic asymmetry of the constituent components.[5] However, intermolecular interactions resulting from an increase in the maleic anhydride (MA) content in an LCST blend of poly(styrene-*co*-maleic anhydride)/poly(methyl methacrylate) (SMA/PMMA) have been observed to dominate the effect of dynamic asymmetry.[1] While the dynamic asymmetry was raised due to the increase in the MA content of the blend, the observed change in the value of θ exhibited a decrease from 2.3° to 0.5° as the MA content was increased from 14% (critical concentration above which the intermolecular interactions dominated the intramolecular interactions in the blend) to 32% in a 50:50 composition of the SMA/PMMA blend. This change of slope is often referred as the binodal temperature of the blend.[1,5,53−55] It is the same temperature around which the turbidity appeared first in the blend as viewed from the window of the SR5 rheometer, during the temperature sweep experiment. Data obtained for the loss tangent, tan δ (plotted alongside the storage and loss modulus in Figure 1), also confirms this proposition. A peak in the loss tangent is clearly observed at the binodal temperature (estimated from the slope change in the G' curve) indicating an energy absorption process preceding phase separation. While the prepeak zone is identified with the miscible region, peak zone refers to the metastable region and the postpeak zone represents the phase-separated region of the phase diagram.[1] The decrease in G' continues above the binodal temperature, albeit at an extremely slow rate, until it touches a minimum only to increase again in magnitude. Such a minimum in the G' curve has often been interpreted as the spinodal temperature of the blend where phase separation is controlled by a different mechanism called the spinodal decomposition and is marked by the growth of domains, rich in the minority and the majority phase of one component leading to a change in the G' behavior.[5] The spinodal temperature estimated from the observed minimum in the G' curve is $T_s \cong 125$ °C for a 50:50 PSD-38K/PVME-23K blend (as shown in Figure 1) where phase-separated domains rich in PSD and PVME are formed. Although the qualitative choice of the minimum temperature should not be unique in this case owing to the reason that the observed range of minima extends well over a decade of temperature, this choice is biased toward the more accurate quantitative estimate of the spinodal temperature using the same data that follows in the text later. Moreover, the magnitude of the upturn and the stretch in the temperature range of the minima for the storage modulus near the critical region are strongly dependent on the dynamic asymmetry (in the T_g of the blend as compared to its pure components) present in the blend. Since a change in the blend composition essentially means a change in the dynamic asymmetry caused by a change in the distance of effective blend T_g from the T_gs of the individual components,[27] the magnitude of the upturn and temperature range of

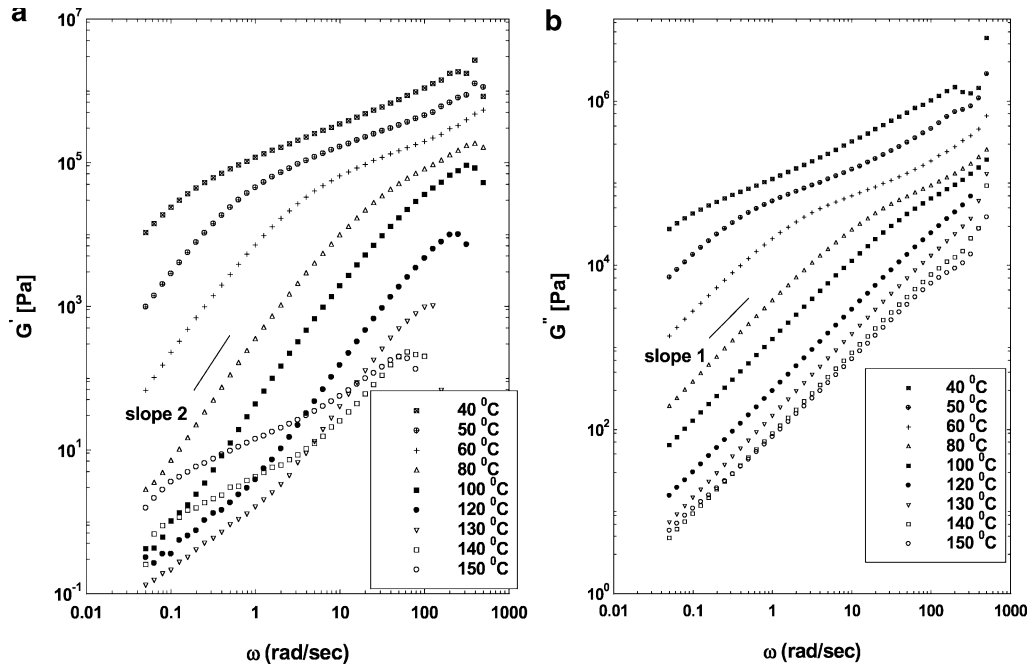

Figure 2. Frequency sweep plots of (a) log G' versus ω and (b) log G'' versus ω, for a 50:50 blend of PSD-38K/PVME-23K, at different temperatures. The scaling laws of $G' \sim \omega^2$ and $G'' \sim \omega^1$ at low frequencies for the homogeneous region (temperatures $T \leq 100$ °C) are shown. An abrupt increase in the magnitude of G' at lower frequencies is clearly visible at high temperatures.

the minima are dependent on the blend composition. A critical composition of the PS/PVME blend resulted in a large (in magnitude) but sharp (shorter range of temperature) change in the storage minima whereas off-critical compositions were marked by the opposite behavior.[5] Different regions (zones 1, 2, and 3) of the blend's phase behavior so identified are depicted in Figure 1. Although such an analysis always contains error, it has been found in good agreement with the experimentally measured values from other methods.[1,5] While the rheological detection of binodal temperature from this method of analysis has near accuracy, boundaries for the region of miscibility (at least on a macroscale) and metastable region are not to be strictly adhered to. Precise estimation of the spinodal temperature by other methods based on shear rheology and quantitative estimation of the same from the data in Figure 1 are described later in the text.

The different regions of the phase behavior having been identified, some inference related to the change in the morphology of the blend can be drawn from the observed response of the viscoelastic data. At low temperatures when the system is still in the homogeneous region, G' decreases with an increase in the temperature caused by an increase in the mobility of the chains as the system moves away from its glass-transition temperature. The ^{2}H NMR spectra of PSD/PVME blends also suggest similar features when the fraction of mobile PS increased compared to the immobile PS with an increase in temperature away from the glass-transition temperature.[56] Further increase in the temperature close to the phase boundary sees a competing effect from thermodynamic forces on the chain mobility.[5] As the temperature approaches critical point, i.e., at small ΔT ($=|T - T_s|$), where T is the experimental temperature and T_s the spinodal temperature), a critical slowdown of the thermodynamic concentration fluctuations occurs. Thus, the thermodynamic forces become dominant, causing an increase in the magnitude of the G' data (observed through the upturn in the G' curve). Because of this balancing effect, the otherwise continuously decreasing G' touches a minimum, only to rise again mainly because of the concentration fluctuation-induced enhancement in the viscoelastic response, leading to the formation of phase-separated domains of PSD and PVME. A similar behavior is observed for the G'' curve near the phase boundary but with a delayed response on the temperature scale. This is because the response to the viscous relaxation in blends always has a time lag to the thermodynamic effect of phase separation resulting in a phase lag between the elastic and viscous components of the stress relaxation. Observations on PS/PVME blends when the reappearance of the phenomenon controlled by mobility forces were observed upon further increase in the temperature[5] could not be confirmed within the range of temperatures studied. We could not make measurements above 160 °C, owing to two reasons: first, because the main aim of this measurement was only to locate the transition region (which is obviously below 160 °C as is clear from the minimum observed in the G' data), and second, because of the restrictions imposed by the experimental conditions as going to higher temperatures often leads to thermal degradation of the blend, and it must be emphasized here that, in order to observe any meaningful effect arising from the thermodynamic forces on the dynamic behavior of the blends, going to a temperature as high as ca. 200 °C only can lead to vital information regarding two-phase behavior of the system. In the case of PS/PVME blends studied by Kapnistos et al.,[5] the highest temperature needed for the pretransitional and the posttransitional study of the blend was low (ca. 130 °C) enough for any measurement to be carried out without thermal degradation of the blend. Since the TGA performed on the blend used in our study exhibited a fairly stable behavior only up to ~155 °C, and also due to the reason that the thermal degradation temperature of the PVME is ca. 150 °C, we stopped our measurement at 160 °C, and this was sufficient to observe the upturn in the G' curve and hence to locate the transition region.

3.2.2. Frequency Sweep Experiment. Dynamical mechanical properties of the blend were measured by the isothermal frequency sweep experiments carried out in a range of temperature, extending from $T_g + 45$ K to $T_g + 155$ K. Plots of storage modulus G' and loss modulus G'' versus frequency, ω, at different temperatures are depicted on a logarithmic scale in Figure 2. Scaling laws obtained for the storage and loss modulii

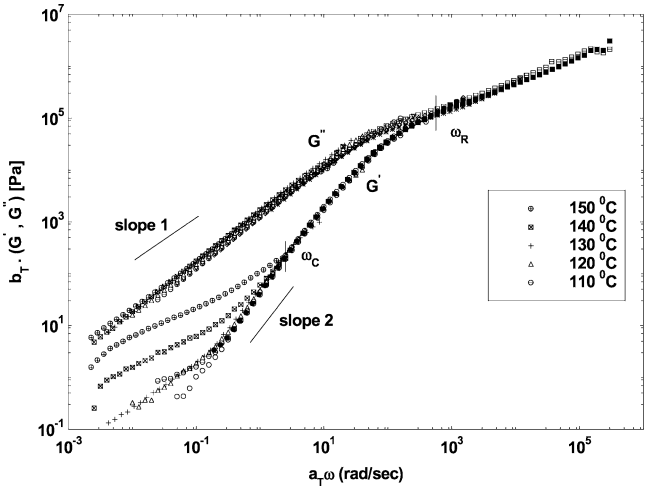

Figure 3. Master curves of storage modulus (G') and loss modulus (G'') for a 50:50 PSD-38K/PVME-23K blend, as a function of frequency ω, at reference temperature 100 °C ($T_{ref} \cong T_g + 105$ K), where a_T and b_T are the frequency-scale and modulus-scale shift factors, respectively. Failure of the tTS principle is clear from the observed deviation in the shifted curve (master curve) at low frequencies. The frequencies corresponding to the longest relaxation time (ω_R) and the onset of thermorheological complexity (ω_c) are shown in the figure. Slopes of the two curves G' and G'' at low frequencies (in the terminal zone) are represented by the solid lines and have values of 2 and 1, respectively. Only the temperatures at which the tTS failure occurs are listed in the figure.

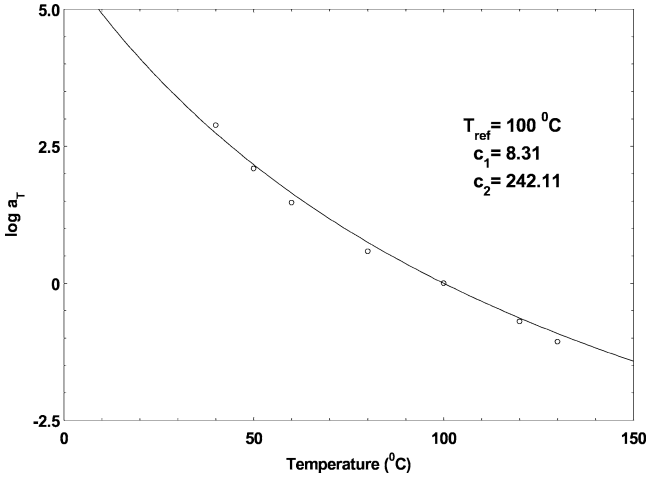

Figure 4. Temperature dependence of the frequency-scale shift factor, a_T (on the logarithmic scale), for the master curve plotted in Figure 3. The curve shown (in the figure) is a fit to eq 2, yielding parametric values of $c_1 = 8.31$ and $c_2 = 242.11$ at a reference temperature of 100 °C.

are $G' \sim \omega^2$ and $G'' \sim \omega^1$ at lower frequencies (in the terminal region) for temperatures $T \leq 100$ °C (as shown in Figure 2). While the G'' data are not much affected, an abrupt increase in the magnitude of the G' data is observed at higher temperatures in the low-frequency region. Following the tTS principle[34] that allows the frequency (ω) dependence of the complex modulus G^* at any temperature T to be determined from a master curve at a reference temperature, which in our case is 100 °C,

$$G^*(\omega;T) = b_T G^*(a_T\omega;T_{ref}) \quad (1)$$

where T_{ref} is the reference temperature and a_T and b_T are the frequency-scale and modulus-scale shift factors required to allow the superposition of the viscoelastic data at temperature T with the data at the reference temperature. The temperature dependence of the frequency-scale shift factor a_T is related to the reference temperature T_{ref} by the semiempirical WLF (Williams−Landel−Ferry) equation,[34]

$$\log a_T = \frac{-c_1(T - T_{ref})}{c_2 + (T - T_{ref})} \quad (2)$$

where c_1 and c_2 are constants. The master curve obtained from the isothermal frequency sweep data of the PSD-38K/PVME-23K blend is depicted in Figure 3. Values of the parameters c_1 and c_2 obtained from fitting eq 2 to the modulus-scale shift factor data, at a reference temperature of 100 °C, are 8.31 and 242.11, respectively, and they (at least the order of the values) are consistent with the values measured by Kapnistos et al.[5] for PS/PVME blends. A fit of the frequency-scale shift factor data to eq 2 is shown in Figure 4. Clearly, the master curve (Figure 3) obtained by shifting the data along the frequency axis shows an anomaly in the G' behavior at lower frequencies. As the temperature increases above 100 °C, an apparent deviation from the terminal slope of the G' curve is observed (at $T = 110$ °C), indicating an anomalous increase in the elasticity of the blend. While the tTS works well for G' and G'' in the terminal region up to temperatures $T \leq 100$ °C (being the miscible region), where the slopes of the curves are 2 and 1, respectively, the superposition fails at $T > 100$ °C, observed immediately after the rheologically determined binodal temperature ($T_b \cong 104$ °C), as seen in the plot of the tTS depicted in Figure 3. Deviations in the terminal slope of the tTS are thought to be due to the thermorheological complexity of the blend. The onset of a thermorheological complexity at higher temperatures (visible at temperatures above T_b) is apparent from the deviations observed in the slope of the master curve at lower frequencies in the terminal region (Figure 3). The thermorheological complexity observed in this region is said to have been caused by the different morphologies formed at different temperatures and undergoing different coarsening kinetics.[5] The frequency corresponding to the longest relaxation time, τ_R ($=1/\omega_R$), and the onset of thermorheological complexity, ω_c ($\tau_c = 1/\omega_c$) marked in Figure 3, have values of 2.63×10^2 rad/s and 2.51 rad/s, respectively. It is therefore clear that the time scale for the onset of thermorheological complexity is much larger than that corresponding to the terminal motion of the chains. The frequency (ω_c) at which the thermorheological complexity appears lies in the terminal region; hence its origin can be attributed to a process associated with the motion of several chains. From the experiments carried out at different compositions of PS/PVME, an increase in the value of τ_c has been reported as a result of increasing polystyrene content in the blend, substantiating the fact that such an increase is, in fact, caused by the formation of polystyrene rich domains.[5] Therefore, the time scale associated with the thermorheological complexity of the blend could be related to the "collective motion" of the chains within the pseudodomains rich in deuterated polystyrene (PSD) formed due to the onset of phase separation.[5] Features of the phase-separated domains formed and observed through the appearance of thermorheological complexity above 100 °C (first observed at 110 °C) are because the system undergoes transition from the miscible to the metastable region (since the rheologically determined binodal temperature is $T_b \cong 104$ °C) of the blend's phase diagram. At 150 °C, the reappearance of the terminal slope of 2 at lower frequencies in the terminal region has been observed similar to the one observed by Kapnistos et al.,[5] in the phase-separated regime. Compared to the G' data, no major deviations are observed in the tTS for the G'' curve, even at temperatures as high as ca. 150 °C, suggesting

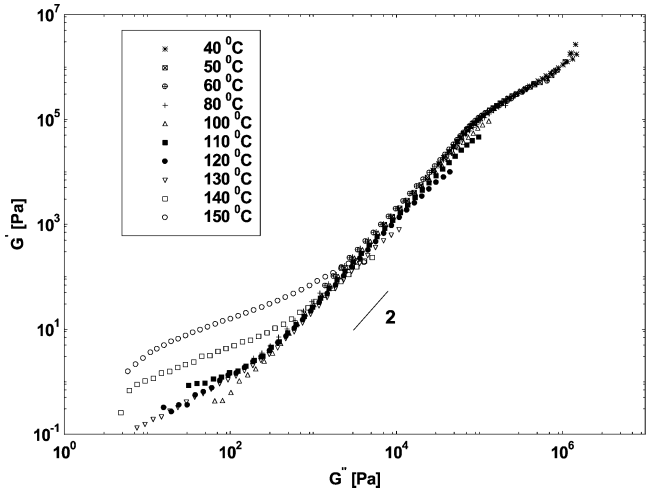

Figure 5. Han plots for a 50:50 PSD-38K/PVME-23K blend at the 10 different temperatures of 40 °C (∗), 50 °C (× in a square), 60 °C (+ in a circle), 80 °C (+), 100 °C (△), 110 °C (■), 120 °C (●), 130 °C (▽), 140 °C (□), and 150 °C (○). The terminal slope of the curves in the homogeneous region is 2 (as shown in the figure). Deviations in the Han plots at temperatures above 100 °C (in the metastable region) are clearly visible in the diagram.

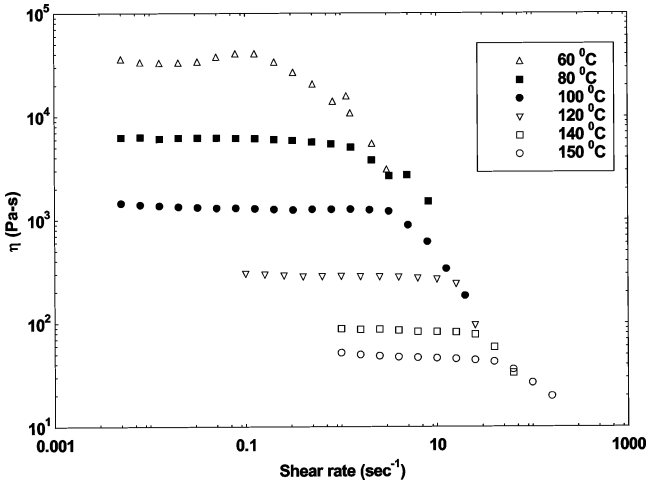

Figure 6. Plot of isothermal viscosity versus shear rate for a 50:50 PSD-38K/PVME-23K blend, over a temperature range covering the homogeneous to the two-phase regime of the blend's phase behavior.

G'' data to be less sensitive to phase transitions than G', similar to the observations in the case of block copolymers.[57] Higher sensitivity of the G' data near the critical phase boundary is mainly due to concentration fluctuation induced stress in the system, which is mostly of elastic origin. In fact, it is this enhanced concentration fluctuation near the phase boundary which indeed is responsible for the deviations observed in the low-frequency regime of the tTS.

A method based on the log−log plot of the storage modulus versus the loss modulus, known as the Han plots,[58] has also been very effective in studying the deviations caused by enhanced concentration fluctuations near the phase boundary. Data obtained from Han plots are often more sensitive to phase changes than the tTS.[59,60] A temperature independence and terminal slope of 2 in the Han plots are the two essential criteria for a phase to be called homogeneous.[59] It has been argued that tTS fails while in the homogeneous regime, near the phase boundary for both LCST and UCST (upper critical solution temperature) types of blends as observed by Kim et al., using similar plots.[61] Figure 5 shows Han plots obtained for a 50:50 composition of PSD-38K/PVME-23K blend, where we clearly observed temperature independence and a slope of 2 in the temperature range of $T \leq 100$ °C, representing the single-phase or the homogeneous region of the PSD-38K/PVME-23K blend. However, the Han plots begin to show temperature dependence at $T \geq 110$ °C, immediately after the binodal temperature ($T_b \cong 104$ °C), characterized by an abrupt increase of the storage modulus in the terminal region. The deviations observed in the Han plots are, in fact, caused by the onset of phase separation at the rheologically determined binodal temperature ($T_b \cong 104$ °C) of the blend. Similar deviations observed by Kim et al.[61] were at temperatures as far as ∼7 °C below the LCST of the PS/PVME and approximately 70 °C above the UCST of a PS/PαMS blend with critical compositions. The reason argued for such failures occurring in the homogeneous region is the presence of microheterogeneity, caused by the dynamical composition fluctuations present near the phase boundary.[61] The difference in the extent of the dynamical composition fluctuations for the two blends (PS/PVME and PS/PαMS) has its origin in the difference between the temperature coefficients of the interaction parameter of PS/PVME and PS/PαMS blend systems. However, no deviation in the temperature dependence of Han plots below (for LCST blend) or above (for UCST blend) the phase boundary were observed in case of off-critical blends.[61] Accordingly, since no deviations were observed in the Han plots below the LCST temperature ($T_b \cong 104$ °C) of 50:50 PSD-38K/PVME-23K blends, such a behavior apparently characterizes the off-critical nature of the blends.

3.3. Viscosity Results. *3.3.1. Rate Sweep Experiment.* The viscosity of a 50:50 PSD-38K/PVME-23K blend, as a function of shear rate at different temperatures, is shown in Figure 6. Experiments carried out over a temperature range of 60 °C to 150 °C included both the single-phase and the two-phase regime of the blend measured at shear rates between 5×10^{-3} and 150 s^{-1}. The viscosity observed at all temperatures resembles that of a simple polymer melt when the system behavior changes from Newtonian to non-Newtonian as the shear rate is increased. It is clear from Figure 6 that the magnitude of the Newtonian viscosity decreases with increase in temperature and the critical shear rate at which a transition from Newtonian to non-Newtonian behavior is observed goes up as the temperature is raised. An important observation that can be made here is that the overall behavior of the Newtonian viscosity as a function of shear rate remains unchanged no matter which part of the phase diagram the system is in. In other words, one can say that no features associated with transition from a homogeneous to a two-phase regime or features specific to the beginning of phase separation could be observed. This is in contrast to viscosity behavior of two-component systems predicted by Onuki.[62] Accordingly, a two-component system near the phase boundary behaves as a suspension of droplets in fluid,[63,64] leading to viscosity enhancement at low shear rates as the critical point is approached. The characteristic of viscosity enhancement near the phase boundary, as argued, is associated with the formation of phase-separated domains. An increase in the shear rate further should see the effects of viscosity enhancement getting nullified only to decrease again until the steady Newtonian value is reached, which is attributed to the breakup of the droplets into smaller sizes due to the application of high shear rate. However, at further high shear rates, the decrease in viscosity continues (beyond the steady Newtonian value) to reach a critical value (the critical shear rate) where the droplets can no longer be detected rheologically, hence causing a sharp decline in the viscosity value, manifesting a non-Newtonian behavior. Such features of viscosity enhancement near the critical phase boundary could not be observed in our experiments

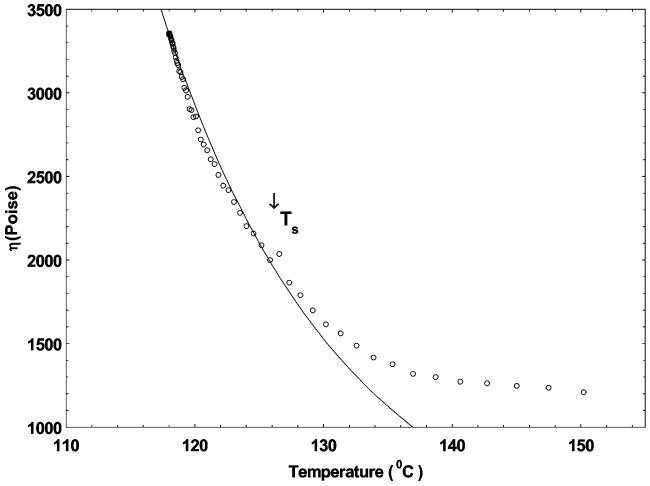

Figure 7. Temperature dependence of viscosity (η) obtained from the temperature sweep experiment at low shear rate (in the linear viscoelastic regime). Deviations from the smoothly varying viscosity−temperature relationship and, hence, a deviation from the expected WLF behavior (shown as fit to eq 3 using the fitting parameters obtained from the WLF fit of the frequency-scale shift factor data earlier) are observed as the system undergoes transition from the homogeneous to the two-phase regime of the phase diagram. The temperature at which deviations begin to appear has been marked as T_s (≈125 °C), the spinodal temperature of the 50:50 PSD-38K/PVME-23K blend.

as opposed to what has been predicted by Onuki.[62] However, an apparent peak visible in the Newtonian region near the critical shear rate at 60 °C is only because of fewer data points in the region, and should not be construed as real.

Similar observations of transition from Newtonian to non-Newtonian have also been reported by Nakatani et al.,[42] on samples of PSD/PVME blends (where the molecular weights of the components were high: $M_w = 4.4 \times 10^5$ and $M_w/M_n = 1.28$ for PSD and $M_w = 1.8 \times 10^5$ and $M_w/M_n = 1.76$ for PVME). However, they observed a smooth decrease in the viscosity between shear rates of 2×10^{-2} and 3.0 s^{-1} (approaching the critical shear rate) for all temperatures from low (single-phase) to high (two-phase) while the system is still in the Newtonian regime. Similar to our experiments, they could not observe the predicted features of viscosity enhancement near the phase boundary. Nevertheless, experiments carried out by them on protonated polystyrene/poly(vinyl methyl ether) (PSH/PVME) blends revealed a viscosity behavior entirely different from the one observed for deuterated polystyrene/poly(vinyl methyl ether) (PSD/PVME) blends, when the observations on PSH/PVME were found to retain the essential features of Onuki's predicted viscosity behavior near the phase boundary. Although they could not exactly match the magnitude of viscosity enhancement predicted by Onuki, the general features of the viscosity enhancement were clearly observed. However, the discrepancy in the viscosity behavior of the polystyrene/poly(vinyl methyl ether) blends in the case when it is protonated and deuterated has not been explained by these authors.

3.3.2. Temperature Sweep Experiment. A plot of the observed viscosity (η) for a 50:50 PSD-38K/PVME-23K blend as a function of temperature at a fixed but vanishing small shear rate of 5×10^{-2} s^{-1} (in the linear viscoelastic regime) near the transition zone is shown in Figure 7. The experimental data shows smooth variation in the viscosity until $T \approx 125$ °C, when a discontinuity in the smoothly varying viscosity−temperature relation is clearly observed above this temperature. This is the same temperature where the minimum in the storage modulus, G', was observed in the dynamic temperature sweep experiments. So the deviation observed above the binodal temperature ($T_b \cong 104$ °C) of the blend can be interpreted as the beginning of phase separation due to spinodal decomposition. Features of discontinuity in the viscosity−temperature relationship for systems undergoing phase separation have also been observed by Wolf et al.[65] (using a viscometric method) and Mazich et al.[66] (using shear rheology when the viscosity was measured at a constant first normal stress), but they interpreted it as the binodal temperature of the system. However, this has not been the case here as the measurements were carried out in a region well past the binodal temperature. The point of discontinuity in the slope of the smoothly varying viscosity curve can therefore only be associated with the spinodal temperature of the 50:50 PSD-38K/PVME-23K blend where the kinetics of phase separation is driven by a mechanism different from the one in the metastable region.

The zero-shear viscosity of a blend in the homogeneous region is predicted by the WLF equation.[34]

$$\log \frac{\eta_0(T)}{\eta_0(T_{ref})} = \frac{-c_1(T - T_{ref})}{c_2 + (T - T_{ref})} \qquad (3)$$

Accordingly, all the data points in the homogeneous region should fall on a single curve well predicted by the shift factor, a_T, in the WLF eq 2. Although the viscosity measured here does not represent the zero-shear viscosity, it must mimic the WLF behavior owing to the reason that the viscosity being measured in the Newtonian region (with $\dot{\gamma} < \dot{\gamma}_{crit}$, where $\dot{\gamma}_{crit}$ is the critical frequency at which the transition from a Newtonian to a non-Newtonian behavior occurs) must have a value nearly equal to the zero-shear viscosity. It must be emphasized here that the rheologically measured viscosity in the linear regime exhibits WLF behavior in the metastable region where the system, at least macroscopically, is homogeneous. The solid line in Figure 7 shows a fit of the experimentally measured viscosity data to the one predicted (for the zero-shear viscosity) by the WLF eq 3 at reference temperature $T_{ref} = 100$ °C (where the values of the constants c_1 and c_2 are taken from the fitting parameters obtained earlier). A clear departure from the WLF behavior is observed at $T \approx 125$ °C, which is the spinodal temperature of the 50:50 PSD-38K/PVME-23K blend. Hence the observed departure of viscosity from the predicted WLF behavior can be regarded as a signature of the spinodal temperature. The method of analysis discussed here serves as an alternative to the existing methods of detecting spinodal temperature rheologically.

4. Discussions

Observations made from the dynamic temperature sweep experiments in the transitional regime of phase separation can be quantified using the expressions derived by Ajji and Choplin[7] for the dynamic storage and loss modulii. An extension to the earlier theory of Fredrickson and Larson[67] for block copolymer melts near the order−order transition to the case of homopolymer blends enabled these authors to derive the critical contribution of the concentration fluctuations to the shear stress for near-critical polymer mixtures using mean-field theory. Following ref 67, the expressions derived for the storage (G') and loss (G'') modulii respectively are

$$G'(\omega) = \frac{k_B T \omega^2}{15\pi^2} \int_0^{k_c} \frac{k^6 S_0^{\,2}(k)}{\omega^2 + 4\bar{\omega}^2(k)} \left[\frac{\partial S_0^{\,-1}(k)}{\partial k^2}\right]^2 dk \qquad (4)$$

$$G''(\omega) = \frac{2k_B T\omega}{15\pi^2}\int_0^{k_c} \frac{k^6 {S_0}^2(k)\bar{\omega}(k)}{\omega^2 + 4\bar{\omega}^2(k)}\left[\frac{\partial {S_0}^{-1}(k)}{\partial k^2}\right]^2 \mathrm{d}k \quad (5)$$

where $\bar{\omega}(k) = k^2 S_0^{-1}(k)\lambda(k)$, $S_0(k)$ is the static structure factor, $\lambda(k)$ is the Onsager coefficient, and k defines the wavevector. Now, the dynamic storage and loss modulii can be calculated either for block copolymers or for binary homopolymer blends by making use of appropriate forms of the structure factor and the Onsager's coefficient. For a homopolymer blend, these expressions can be derived using (i) the form of the static structure factor derived by deGennes[68] with the aid of the random phase approximation (RPA) based on the mean-field approach,

$$\frac{1}{S_0(k)} = \frac{1}{\phi N_1 g_1(k)} + \frac{1}{(1-\phi)N_2 g_2(k)} - 2\chi \quad (6)$$

where ϕ is the volume fraction of polymer 1, N_i is the number of statistical segments, and $g_i(k)$ is the Debye function, and (ii) the form of Onsager coefficient, $\lambda(k)$, proposed by Binder,[69]

$$\frac{1}{\lambda(k)} = \frac{1}{\phi {a_1}^2 W_1 g_1(k)} + \frac{1}{(1-\phi){a_2}^2 W_2 g_2(k)} \quad (7)$$

where a_i is the statistical segment length of the species i and W_i the rate of reorientation of a segment of polymer, a component of the blend, into the matrix of another component defined by

$$W_i = 3\pi k_B T/\zeta_i \quad (8)$$

where ζ_i is the monomeric friction coefficient. Ajji and Choplin[7] used the above expressions (eq 6 to eq 8) to recalculate the form of dynamic storage and loss modulii defined in eqs 4 and 5 in the following manner. In the homogeneous region near the critical point, eq 6 and eq 7 can be approximated by introducing an expansion of the Debye function, $g_i(k)$, to the first term, resulting in the following form of expressions for $S_0(k)$ and $\lambda(k)$:

$${S_0}^{-1}(k) = 2(\chi_s - \chi) + \left[\frac{1}{\phi N_1}\frac{{R_{g_1}}^2}{3} + \frac{1}{(1-\phi)N_2}\frac{{R_{g_2}}^2}{3}\right]k^2 \quad (9)$$

$$\lambda^{-1}(k) = \frac{1}{\phi {a_1}^2 W_1} + \frac{1}{(1-\phi){a_2}^2 W_2} + \left[\frac{{R_{g_1}}^2}{\phi a_1 W_1} + \frac{{R_{g_2}}^2}{(1-\phi)a_2 W_2}\right]k^2 \quad (10)$$

where χ_s is the value of the interaction parameter at the spinodal. Using eqs 9 and 10 in eqs 4 and 5, and performing the integration with proper approximations in the limit when χ tends to χ_s, the form of expressions obtained for the dynamic storage and loss modulii in the terminal one-phase region near the critical point are

$$G'(\omega) = \frac{k_B T\omega^2}{1920\pi}\left[\frac{1}{3}\left\{\frac{{R_{g_1}}^2}{\phi N_1} + \frac{{R_{g_2}}^2}{(1-\phi)N_2}\right\}\right]^{1/2} \times \left[\frac{1}{\phi {a_1}^2 W_1} + \frac{1}{(1-\phi){a_2}^2 W_2}\right]^2 [2(\chi_s - \chi)]^{-5/2} \quad (11)$$

$$G''(\omega) = \frac{k_B T\omega}{240\pi}\left[\frac{1}{3}\left\{\frac{{R_{g_1}}^2}{\phi N_1} + \frac{{R_{g_2}}^2}{(1-\phi)N_2}\right\}\right]^{-1/2} \times \left[\frac{1}{\phi {a_1}^2 W_1} + \frac{1}{(1-\phi){a_2}^2 W_2}\right][2(\chi_s - \chi)]^{-1/2} \quad (12)$$

where R_{g_i} is the radius of gyration defined as ${R_{g_i}}^2 = N_i {a_i}^2/6$. Using eqs 11 and 12, the ratio $G'(\omega)/G''^2(\omega)$ can be calculated where, with an appropriate substitution for the values of the defined parameters, one can eliminate the monomeric friction coefficients to get an expression that has no explicit frequency dependence:

$$\frac{G'}{G''^2} = \frac{30\pi}{k_B T}\left\{\frac{{a_1}^2}{36\phi} + \frac{{a_2}^2}{36(1-\phi)}\right\}^{3/2}(\chi_s - \chi)^{-3/2} \quad (13)$$

However, the point must be emphasized that such an expression is valid only for the terminal response (near the critical region) where the dynamic storage and loss modulii have a scaling behavior of $G' \sim \omega^2$ and $G'' \sim \omega^1$, respectively. The behavior of the correlation length of a binary polymer blend near the critical region is predicted by the RPA to be

$$\xi = \frac{a'}{6}[\phi(1-\phi)(\chi_s - \chi)]^{-1/2} \quad (14)$$

where a' is the characteristic length, related to the individual segment lengths, a_1 and a_2, by the relation

$$\frac{a'^2}{\phi(1-\phi)} = \frac{{a_1}^2}{\phi} + \frac{{a_2}^2}{(1-\phi)} \quad (15)$$

Therefore, the form of expression for the correlation length becomes

$$\xi = \left[\frac{k_B T}{30\pi}\frac{G'}{G''^2}\right]^{1/3}\frac{1}{\phi(1-\phi)} \quad (16)$$

Thus, the correlation length as a function of temperature can be measured near the critical point directly from shear rheological data obtained from the dynamic temperature sweep experiments. Although both the expressions used in eq 14 and eq 16 appear to give the same information, the limitations of using eq 16 to calculate the fluctuation correlation length must be explained. While eq 14, a well-established RPA (random phase approximation) result, can be used to calculate exactly the value of ξ both near and far from the critical region of the phase diagram, eq 16 is an empirical way of calculating the same from the viscoelastic response data valid only near the critical region. Equation 13 leads to an important observation, when a linear dependence of $(G''^2/G'T)^{2/3}$ versus $1/T$ is predicted for the blends of PSD and PVME, assuming $\chi = A + B/T$ behavior of the interaction parameter. The spinodal temperature, T_s, can be estimated from the intercept of the line with the $1/T$ axis. Such a behavior obtained from the data of dynamic temperature sweep experiments on 50:50 PSD-38K/PVME-23K blend is shown in Figure 8. The figure clearly shows deviation on both sides of the linear regime at temperatures away from the critical region since the original theory developed on the basis of mean-field approximation here accounts for the one-phase region close to the critical point only. The estimated spinodal temperature from the intercept is $T_s = 124.6$ °C. However, the T_s estimated from this method is bound to have an error of 1 to 2 °C as the analysis is based on the true selection

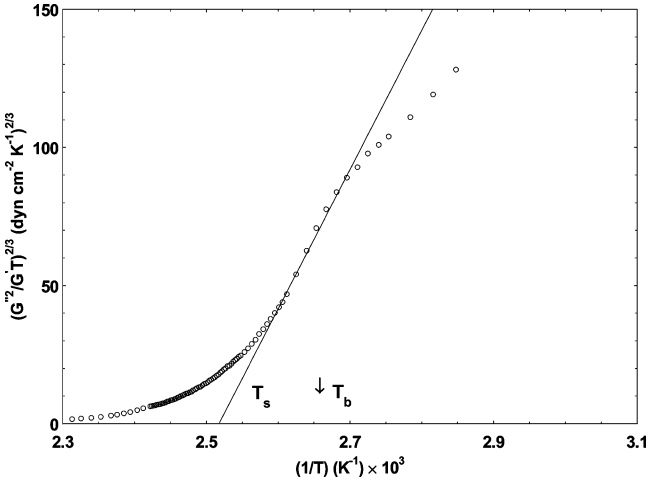

Figure 8. Estimation of spinodal temperature from the quantitative evaluation of the viscoelastic response of a 50:50 PSD-38K/PVME-23K blend, near the phase boundary. The spinodal and the cloud point temperatures are indicated in the figure as intercept and vertical arrow, respectively.

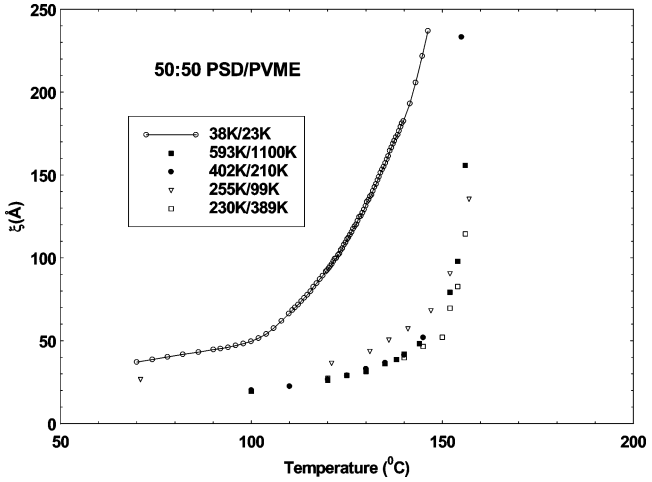

Figure 9. Temperature dependence of the correlation length obtained quantitatively from the isochronal dynamic temperature sweep data of storage and loss modulus in Figure 1. The correlation length (data points only) obtained from the SANS data of 50:50 PSD/PVME blends (available from other literature sources) are also plotted along with our data (joined curve) for comparison. The molecular weight ratios of individual blends are listed in the figure.

of linear range in the curve. The validity of the estimated correlation length from this method has already been tested, and the estimates have been found in reasonable agreement with the experimentally obtained values from SANS.[7] A plot of the correlation lengths estimated from eq 16 at different temperatures near the spinodal is shown in Figure 9 as a joined curve. The values of the correlation lengths obtained in our case have been compared with similar data (from other literature sources)[43,44] obtained from SANS studies of 50:50 PSD/PVME blends of varying component molecular weights in Figure 9. The SANS-obtained correlation lengths are marked only as data points with their component molecular weights listed in Figure 9. The order of the rheologically obtained correlation lengths is almost the same as the order of lengths obtained from SANS except for the fact that all the spinodal temperatures obtained from the latter have slightly higher values and the transition is rather sharp. This could be attributed to the fact that the SANS data quoted from the literature are from blends of high polymers, i.e., molecular weights of both the components (PSD and PVME) are very high as compared to the one we have used leading to the suppression of concentration fluctuations at lower temperatures, in general. The temperature dependence of the correlation length obtained from 50:50 PSD-38K/PVME-23K blend clearly shows divergence around 140 °C to 150 °C, and the inflection point in this curve can be thought to represent the spinodal temperature ($T_s \cong 125$ °C) of the blend which is marked by the formation of a giant interconnected network structure of polymer chains due to phase separation. The divergence observed in the correlation length, typically associated with the phase separating binary systems, is primarily caused by the enhanced concentration fluctuation contribution to the viscoelastic response of $G'$and G'' near the critical region (close to the spinodal temperature of the blend). Hence, this method of estimation for the correlation length is not valid in the regions far away from the critical region.

5. Conclusions

In summary, we have presented a detailed rheological investigation of an LCST blend of PSD-38K/PVME-23K near the critical region. The phase behavior of the blend and region of miscibility are determined experimentally on the basis of shear rheological measurements. Three regions of the phase behavior, namely, miscible (zone 1; $T \lesssim 96$ °C), metastable (zone 2; 96 °C $\lesssim T \lesssim$ 125 °C), and phase-separated (zone 3; $T \gtrsim 125$ °C), are identified from the dynamic temperature sweep measurements. While the binodal temperature ($T_b \cong 104$ °C) is estimated from the observed change in the slope of G' behavior and the peak in the loss tangent curve, miscible and phase-separated regions were only identified asymptotically as the prepeak and after-peak zones in the tan δ curve. More precise quantitative estimation of the spinodal temperature (T_s = 124.6 °C) from the same data was done using the mean-field approach. Such an estimate of the phase boundary carried out rheologically has been found in good agreement with the results obtained from other conventional methods; e.g., the spinodal temperature obtained from SANS studies of this blend is 125.4 °C.[70] A novel method for the estimation of the spinodal temperature based on the viscosity measurement has also been suggested. Through a combination of the observed discontinuity in smoothly varying viscosity−temperature relationship and its noncompliance with the predicted WLF behavior, the spinodal temperature is located using the temperature sweep experiment (in the linear regime). However, the two suggested methods of determining spinodal temperature lead to a unique complexity arising from the difference in the observations made from the oscillatory and continuous shear measurements. A direct consequence of the tTS failure observed through the storage and loss modulii is that the complex viscosity, which is a function of G' and G'', must also exhibit similar behavior leading to the determination of the binodal temperature. However, failure of the observed viscosity (measured in the continuous shear mode) to comply with the WLF equation has led to the spinodal temperature, which means it differs significantly from the complex viscosity. This is possible only when the Cox−Merz rule,[71] which relates the linear dynamic modulus as a function of frequency to the steady shear flow viscosity as function of shear rate, fails. Even if one accepts the argument of the Cox−Merz rule failure, it is difficult to resolve the difference between the behavior of complex viscosity, which is a linear viscoelastic function, and that of the shear viscosity, which then is a nonlinear viscoelastic function using these data only. The effect of oscillatory and steady flow on the thermodynamics of the system needs to be studied in detail before anything conclusive is said on these aspects of the viscoelastic response behavior.

Another remarkable observation is that the difference between the binodal and the estimated spinodal temperatures is approximately 20 °C, which is quite high even if one considers the blends to have an off-critical composition. However, in yet another investigation by Kim et al., difference of the same order between the binodal and spinodal temperatures has been reported for a 50:50 PS/PVME off-critical blend when the T_s was determined from the plots of $(G''^2/G'T)^{2/3}$ versus $1/T$.[72] The reason argued for such a large difference between the two temperatures is that spinodal temperature determined from the mean-field approximation method is only more reliable for critical composition than the off-critical compositions as the theory was originally developed for the former.

The phase behavior of the blend in the transitional regime has been studied mainly by the viscoelastic response of the system during dynamic temperature sweep experiments. The tTS, which works reasonably well in the homogeneous region, exhibits failure in the metastable region, marked by an abrupt increase in the storage modulus at low frequencies. Han plots also proved this proposition by exhibiting temperature dependence and departure from terminal slope of 2 in this temperature range. The thermorheological complexity of the blend observed near the phase boundary is caused by a process that has a time scale much higher than the terminal relaxation of the chains caused by the formation of phase-separated domains rich in PSD and PVME in the metastable region. At higher temperatures, above the spinodal, the kinetics is controlled by a different mechanism (than the metastable region) related to the evolving morphologies at different temperatures.

While the observations made on the blends of PSD/PVME retain the essential features of the PS/PVME blends' phase behavior, viscosity measured near the critical phase boundary differed significantly. The observed behavior of the viscosity for the PSD/PVME blends does not obey Onuki's predicted behavior of two-component systems near phase boundary, which generally holds true for the blends of PS/PVME.[62] The correlation length estimated from the enhanced concentration fluctuation contribution to the viscoelastic response of the storage and loss modulus near the critical region exhibited divergence, a behavior generally predicted for the binary systems undergoing phase separation.

Acknowledgment. Financial support of research from Engineering and Physical Sciences Research Council is acknowledged with gratitude. We thank Lian Hutchings for synthesizing the deuterated polystyrene used in the experiments and having carried out GPC on the polymer samples used in this work. Thank is also due to Dave Hunter, who made the DSC runs over the samples. We also thank João Cabral for providing his expertise on various aspects of technical problems related to the experiments and helpful suggestions regarding the sample preparation techniques. J.S. also thanks Julia S. Higgins for fruitful discussion on various aspects of data analysis.

References and Notes

(1) Chopra, D.; Kontopoulou, M.; Vlassopoulos, D.; Hatzikiriakos, S. G. *Rheol. Acta* **2002**, *41*, 10. Chopra, D.; Vlassopoulos, D.; Hatzikiriakos, S. G. *J. Rheol.* **2000**, *44*, 27.

(2) Pathak, J. A.; Colby, R. H.; Kamath, S. Y.; Kumar, S. K.; Stadler, R. *Macromolecules* **1998**, *31*, 8988.

(3) Pavawongsak, S.; Higgins, J. S.; Clarke, N.; McLeish, T. C. B.; Peiffer, D. G. *Polymer* **2000**, *41*, 757.

(4) Pathak, J. A.; Colby, R. H.; Floudas, G.; Jerome, R. *Macromolecules* **1999**, *32*, 2553.

(5) Kapnistos, M.; Vlassopoulos, D.; Anastasiadis, S. H. *Europhys. Lett.* **1996**, *34*, 513. Kapnistos, M.; Hinrichs, A.; Vlassopoulos, D.; Anastasiadis, S. H.; Stammer, A.; Wolf, B. A. *Macromolecules* **1996**, *29*, 7155.

(6) Schneider, H. A.; Wirbser, J. *New Polym. Mater.* **1990**, *2*, 149.

(7) Ajji, A.; Choplin, L. *Macromolecules* **1991**, *24*, 5221.

(8) Stadler, P. F.; Feltas, L. L.; Krieger, V.; Klotz, S. *Polymer* **1988**, *29*, 1643.

(9) Caville, J. Y.; Perez, J.; Jourdan, C.; Johari, G. P. *J. Polym. Sci., Part B: Polym. Phys.* **1987**, *25*, 1847.

(10) Paul, D. R., Newman, S., Eds. *Polymer Blends*; Academic Press: New York, 1978.

(11) Olabisi, O.; Robeson, L. M.; Shaw, M. T. *Polymer-Polymer Miscibility*, Academic Press: New York, 1979.

(12) Nishi, T.; Kwei, T. K. *Polymer* **1975**, *16*, 285.

(13) Nishi, T.; Wang, T. T.; Kwei, T. K. *Macromolecules* **1975**, *8*, 227.

(14) Hashimoto, T.; Kumaki, J.; Kawai, T. *Macromolecules* **1983**, *16*, 641.

(15) Hashimoto, T.; Itakura, M.; Hasegawa, H. *J. Chem. Phys.* **1986**, *16*, 6118.

(16) David, D. D.; Kwei, T. K. *J. Polym. Sci., Polym. Phys. Ed.***1980**, *18*, 2337.

(17) Okada, M.; Han, C. C. *J. Chem. Phys.* **1986**, *85*, 5317.

(18) Han, C. C.; Okada, M.; Muroga, Y.; Bauer, B. J.; Tran-cong, Q. *Polym. Eng. Sci.* **1986**, *26*, 1208.

(19) Shibayama, M.; Yang, H.; Stein, R. S.; Han, C. C. *Macromolecules* **1985**, *18*, 2179.

(20) Gerald, H.; Higgins, J. S.; Clarke, N. *Macromolecules* **1999**, *32*, 5411.

(21) Janssen, S.; Schwahn, D.; Mortensen, K.; Springer, T. *Macromolecules* **1993**, *26*, 5587.

(22) Schwahn, D.; Mortensen, K.; Yee-Madeira, H. *Phys. Rev. Lett.* **1987**, *58*, 1544.

(23) Fernandez, M. L.; Higgins, J. S.; Richardson, S. M. *Trans. Inst. Chem. Eng.* **1993**, *71A*, 293.

(24) Hindawi, I. A.; Higgins, J. S.; Weiss, R. A. *Polymer* **1992**, *33*, 2522.

(25) Mani, S.; Malone, M. F.; Winter, H. H. *Macromolecules* **1992**, *25*, 5671.

(26) Katsaros, J. D.; Malone, M. F.; Winter, H. H. *Polym. Eng. Sci.* **1989**, *29*, 1434.

(27) Tanaka, H. *Phys. Rev. Lett.* **1996**, *76*, 787.

(28) Shiomi, T.; Hamada, F.; Nasako, T.; Yoneda, K.; Imai, K.; Nakajima, A. *Macromolecules* **1990**, *23*, 229.

(29) Tsujita, Y.; Kato, M.; Kinoshita, T.; Takizawa, A. *Polymer* **1992**, *33*, 773.

(30) Yang, H.; Shibayama, M.; Stein, R. S.; Shimizu, N.; Hashimoto, T. *Macromolecules* **1986**, *19*, 1667.

(31) Han, C. C. *Rubber Chem. Technol.* **1990**, *63*, 98.

(32) Hadziioannou, G.; Stein, R. S. *Macromolecules* **1984**, *17*, 567.

(33) Kumar, S. K.; Colby, R. H.; Anastasiadis, S. H.; Fytas, G. *J. Chem. Phys.* **1996**, *105*, 3777.

(34) Ferry, J. D. *Viscoelastic Properties of Polymers*, 3rd ed.; Wiley: New York, 1980.

(35) Arendt, B. H.; Krisnamoorti, R.; Kornfield, J. A.; Smith, S. D. *Macromolecules* **1997**, *30*, 1127. Arendt, B. H.; Kannan, R. M.; Zewail, M.; Kornfield, J. A.; Smith, S. D. *Rheol. Acta* **1994**, *33*, 322.

(36) Chung, G. C.; Kornfield, J. A.; Smith, S. D. *Macromolecules* **1994**, *27*, 964. Chung, G. C.; Kornfield, J. A.; Smith, S. D. *Macromolecules* **1994**, *27*, 5729.

(37) Zawada, J. A.; Fuller, G. G.; Colby, R. H.; Fetters, L. J.; Roover, J. *Macromolecules* **1994**, *27*, 6861.

(38) Roovers, J.; Toporowski, P. M. *Macromolecules* **1992**, *25*, 1096. Roovers, J.; Toporowski, P. M. *Macromolecules* **1992**, *25*, 3454.

(39) Roland, C. M.; Ngai, K. L. *Macromolecules* **1991**, *24*, 2261.

(40) Zawada, J. A.; Fuller, G. G.; Colby, R. H.; Fetters, L. J.; Roover, J. *Macromolecules* **1994**, *27*, 6851.

(41) Schwahn, D.; Janssen, S.; Springer, T. *J. Chem. Phys.* **1992**, *97*, 8775.

(42) Nakatani, A. I.; Kim, H.; Takahashi, Y.; Matsushita, Y.; Takano, A.; Bauer, B. J.; Han, C. C. *J. Chem. Phys.* **1990**, *93*, 795.

(43) Han, C. C.; Bauer, B. J.; Clark, J. C.; Muroga, Y.; Matsushita, Y.; Okada, M.; Tran-cong, Q.; Chang, T. *Polymer* **1988**, *29*, 2002.

(44) Shibayama, M.; Yang, H.; Stein, R. S.; Han, C. C. *Macromolecules* **1985**, *18*, 2179.

(45) Herkt-Maetzky, C.; Schelten, J. *Phys. Rev. Lett.* **1983**, *51*, 896.

(46) Halary, J. L.; Ubrich, J. M.; Monnerie, L.; Yang, H.; Stein, R. S. *Polym. Commun.* **1985**, *26*, 73.

(47) Similar degree of superheating here means the blends are quenched to temperatures, equidistant from their respective spinodal temperatures.

(48) Matsushita, Y.; Furuhashi, H.; Choshi, H.; Noda, I.; Nagasawa, M.; Fujimoto, T.; Han, C. C. *Polym. J.* **1982**, *14*, 489.

(49) Stoelting, J.; Karasz, F. E.; MacKnight, W. J. *Polym. Eng. Sci.* **1970**, *10*, 123.

(50) Molnar, A.; Eisenberg, A. *Macromolecules* **1992**, *25*, 5774.
(51) Kaplan, D. S. *J. Appl. Polym. Sci.* **1976**, *20*, 2615.
(52) Masson, J. F.; Manley, R. J. *Macromolecules* **1992**, *25*, 589.
(53) Vlassopoulos, D. *Rheol. Acta* **1996**, *35*, 556. Vlassopoulos, D.; Koumoutsak, A.; Anastasiadis, S. H.; Hatzikiriakos, S. G.; Englezos, P. *J. Rheol.* **1997**, *41*, 739.
(54) Chopra, D.; Vlassopoulos, D.; Hatzikiriakos, S. G. *J. Rheol.* **1998**, *42*, 1227.
(55) Jeon, H. S.; Nakatani, A. I.; Han, C. C.; Colby, R. H. *Macromolecules* **2000**, *33*, 9732.
(56) Tezuka, A.; Takegoshi, K.; Hikichi, K. *J. Mol. Struct.* **1995**, *355*, 1.
(57) Bates, F. S. *Macromolecules* **1984**, *17*, 2607. Bates, F. S.; Rosedale, J. H.; Fredrickson, G. H. *J. Chem. Phys.* **1990**, *92*, 6255.
(58) Han, C. D.; Lem, K. W. *Polym. Eng. Rev.* **1982**, *2*, 135.
(59) Han, C. D.; Baek, D. M.; Kim, J. K.; Ogawa, T.; Sakamoto, N.; Hashimoto, T. *Macromolecules* **1995**, *28*, 5043. Han, C. D.; Baek, D. M.; Kim, J. K. *Macromolecules* **1990**, *23*, 561. Han, C. D.; Kim, J. K. *Macromolecules* **1989**, *22*, 4292. Han, C. D.; Kim, J. *J. Polym. Sci., Part B: Polym. Phys.* **1987**, *25*, 1741. Han, C. D.; Jhon, M. S. *J. Appl. Polym. Sci.* **1986**, *32*, 3809.
(60) Nesarikar, A. *Macromolecules* **1995**, *28*, 7207.
(61) Kim, J. K.; Lee, H. H.; Son, H. W.; Han, C. D. *Macromolecules* **1998**, *31*, 8566.
(62) Onuki, A. *Phys. Rev. A* **1987**, *35*, 5149.
(63) Roscoe, R. *J. Fluid Mech.* **1967**, *28*, 273.
(64) Chaffey, C. E.; *Colloid Polym. Sci.* **1977**, *255*, 691.
(65) Wolf, B. A.; Sezen, M. C. *Macromolecules* **1977**, *10*, 1010.
(66) Mazich, K. A.; Carr, S. H. *J. Appl. Phys.* **1983**, *54*, 5511.
(67) Fredrickson, G. H.; Larson, R. G. *J. Chem. Phys.* **1987**, *86*, 1553.
(68) deGennes, P. G. *Scaling Concepts in Polymer Physics*; Cornell University Press: Ithaca, New York, 1979.
(69) Binder, K. *J. Chem. Phys.* **1983**, *79*, 6387.
(70) To be published.
(71) Cox, W. P.; Merz, E. H. *J. Polym. Sci.* **1958**, *28*, 619.
(72) Kim, J. K.; Son, H. W. *Polymer* **1999**, *40*, 6789.